SOVIET PHYSICS USPEKHI VOLUME 13, NUMBER 1 JULY-AUGUST 1970

530.145

ELECTRONIC ENERGY SPECTRA AND THE EQUATION OF STATE OF SOLIDS AT HIGH PRESSURES AND TEMPERATURES

A. I. VOROPINOV, G. M. GANDEL'MAN, and V. G. PODVAL'NYĬ

Usp. Fiz. Nauk 100, 193-224 (February, 1970)

I. GENERAL PHYSICAL PRINCIPLES

1. Brief Summary of the Fundamental Results

THE purpose of the present review is to describe in detail the quantum-mechanical theory and the results of calculations of electronic energy spectra and the equation of state of crystalline solids in a wide range of pressures and temperatures. The described method makes it possible to consider all pressures, as well as temperatures below 100,000°K.

At very high pressures (more than 100 million atm) and temperatures (higher than 0.5 keV), good results can be obtained for the equation of state by the statistical Thomas-Fermi and Thomas-Fermi-Dirac theories, which constitute a quasi classical approximation to the self-consistent-field method. These theories have been perfected in the well known papers of Feynman, Metropolis, and Teller[1], and of Latter[2]. At the same time, it is well known that the results of calculations by the statistical theory differ noticeably from the experimental data for the dependence of the pressure on the density in the region of small degrees of compression $\delta = \rho/\rho_0$ (ρ—density of the compressed substance, ρ_0—normal density of the substance).

Kirzhnits[3,4] and Kalitkin[5] succeeded in constructing a Thomas-Fermi model with allowance for quantum and exchange corrections (the TFC method). The calculations performed by this procedure have noticeably improved the agreement with the experimental data obtained by Al'tshuler et al.[6] by investigating the properties of substances with shock waves. From other theoretical investigations, dealing with matter at high pressures, mention should be made of the work of Abrikosov[7] and Carr[8] on hydrogen.

At normal densities, and also at small compressions ($\delta \sim 1-2$), the TFC model becomes, generally speaking, useless, since in this region it is impossible to neglect the shell structure of the atoms constituting the crystal lattice. In addition, in the derivation of the equations for the quantum corrections in the TFC model it was assumed that the corrections are small, and the calculation resulted in large correction terms. Indeed, statistical methods are incapable of explaining the sharp fluctuations of the normal densities of substances over the periodic system, the possible deviations of the pressure curve $p(\rho)$ from smoothness, the electronic-type phase transitions, the anomalously large values of the electronic specific heats of transition metals, etc.

It should be noted that the feasibility of phase transitions that depend on the redistribution of the electrons among the shells was predicted by Fermi and traced theoretically by Sternheimer in cesium[9].

I. M. Lifshitz[10] investigated the anomalies of the electronic coefficient of compressibility and other electronic characteristics of metals at large pressures near the "electronic-transition" singular point connected with the change of the topology of the Fermi surface as the latter is continuously deformed.

The need arose for a more accurate quantum-mechanical investigation of the electronic structure of a solid at different compressions. Since the initial purpose of our investigation was to obtain data on the equation of state in solids (we are referring to the pressure, electronic specific heat, the distribution of the electron density, etc., i.e., quantities that apparently depend little on the true form of the cell), it was natural to make some simplifying assumptions. We therefore did not consider molecular and valent crystals having complicated structures.

We begin with the closest packing, since at high pressures the complex structures have a tendency to go over into structures with closest packing. As always in such cases, the band theory is used, based on two assumptions: first, it is assumed that the crystal can be represented by an ideal periodic structure with immobile nuclei; second, it is assumed that each electron moves independently in a periodic potential, which takes into account on the average the interaction between the electron and remaining crystal (the one-electron approximation). The complete wave function of the system of electrons is then expressed in terms of the one-electron wave functions, each of which is written as a product of a spatial part and a spin part.

The one-electron wave functions are determined by using the Hartree approximation, i.e., the influence of the exchange interaction on the wave function is disregarded. The Hartree equation for the wave function of the electron is the Schrödinger equation in a self-consistent periodic potential $V(r)$. In the general case $V(r)$ describes the interaction of a given electron both with the nucleus and with the electrons of the cell under consideration, and with the nuclei and electrons of other cells.

For crystals with a high degree of symmetry (body-centered lattice, face-centered lattice), the contribution made to the potential by electrons of cells other than the given cell is approximately cancelled by the contribution of the nuclei*. It suffices therefore to consider the Hartree equation in a given cell. It must be borne in mind here that the potential itself depends on the sought wave functions (for bands of sufficient

*Seitz [11] estimated the contribution of the deviation from spherical symmetry in the charge distribution for a body-centered lattice of ions with a smeared homogeneous distribution of the negative charges and obtained an exceedingly negligible correction to the energy.

width, considering the equation for the one-electron function with given k, we take into account in the potential electrons with arbitrary k′, without discarding the contribution of the narrow region near k′ = k, since this contribution is negligibly small.)

It is known that solutions in a periodic potential should satisfy the Bloch conditions, which follow from the translational symmetry of the crystal. Thus, the complete Hartree problem in a crystal reduces to a solution of an equation in one cell with periodic boundary conditions. It is necessary to bear in mind that even when the potential is specified, the solution of the Schrödinger equation for different crystal structures is a very laborious problem, entailing a large volume of computational work. Recently, many approximate methods were developed for the solution of the wave equation in a crystal (see the reviews[12-14]). We emphasize that in these papers the dependence of the pressure on the density was not calculated. The calculations were performed for normal density of solids, and the potential was constructed in accordance with the data of calculations for isolated atoms, obtained with the aid of the Hartree and Hartree-Fock approximations. These complicated methods are important for the study of the structure of the Fermi surface of metals and semiconductors for different types of crystal lattices.

All this is important for the solution of subtle problems connected with electric and magnetic properties. However, for strongly compressed metals, the Hartree potentials of isolated atoms cannot be used, since they are remote from the true potential acting on the electron in a compressed crystal. In crystals with a high degree of symmetry, at high pressures, there should be realized any one of the close-packing lattices. In this case, the unit cell is close to a sphere. Therefore to calculate the pressure in the compressed crystal we consider it advisable to use the Wigner-Seitz method of spherical cells (the unit cell is replaced by an equivalent sphere). This well known approximation, which does not provide great accuracy in the description of the energy band structure of the crystal and of the Fermi surface, turned out to be very useful for our purposes since, on the one hand, it simplifies greatly the calculations and uncovers possibilities for large scale computation, and, on the other hand, it does not spoil a number of singularities in the behavior of $p(\rho)$, in the character of the filling of the bands, or in the behavior of the electronic specific heat, the results in many cases being in good agreement with the experimental data.

The wave functions and the potential are determined in the Hartree approximation by the method of successive approximations. The initial approximation most frequently is the Thomas-Fermi potential of the compressed atom. From the obtained wave functions of the initial approximation, one determines the effective potential of the next approximation. The process of successive approximations terminates when the next potential differs little from the preceding one. It should be noted that the aforementioned iteration process (simple iterations) diverges as a rule. It is therefore necessary to use special methods for improving the convergence of the iteration process. In addition, the calculation starts with an improved initial approximation of the potential. Specifying the density of the substance, the atomic weight A, and the atomic number Z, we obtain after the end of the process of successive approximations the "self-consistent" potential and the wave function of the electrons, and also the distribution of the electron density and the electron occupation numbers in the energy bands. The possibility of calculating the pressure makes it possible to get along without using experimental data and to determine the normal density of the matter theoretically (at p = 0). Whereas the statistical theory leads to a monotonic increase of the normal density of substances with increasing Z, the quantum-mechanical theory represents correctly the oscillations of the normal density. For example, for potassium the calculated normal density is 0.68, as against 3.95 g/cm^3 given by the statistical theory (the experimental normal density is ρ_0 = 0.865 g/cm^3). For iron, the difference is smaller, 6.03 g/cm^3 calculated against 5.15 g/cm^2 according to TFC (experimental—7.8 g/cm^3).

It was already noted that one of the results of the calculation is the determination of the energy band structure for different compressions δ, i.e., the dependence of the energy E_i on the quasimomentum k. In the spherical-cell approximation the energy depends only on the absolute value of the quasimomentum k. After obtaining the electron energy spectrum $E_i(k)$, the bands are filled up to the maximum Fermi energy E_F, starting from the given number of electrons Z.

In this problem, the quasimomentum k has a preferred direction. Therefore the projection of the momentum on the k direction is a conserved quantity, unlike the total angular momentum, which is not conserved. By virtue of this, the wave function is a superposition of harmonics with different values of the orbital angular momentum, but with the same value of m. It is reasonable, however, to assign for classification purposes an index l_0 to a definite energy band, taking this to mean the value of l of the level to which the band goes over as $\rho \to 0$. We shall henceforth use the band designations 4s, 3d, 3p, 4f, etc. precisely in this sense. Each band splits into subbands with different values of $m \leq l_0$, so that the index i denotes the aggregate of the three quantum numbers nl_0m. (We note that the states m and −m are physically equivalent, so that we can confine ourselves only to the case $m \geq 0$). For example, the 3d band splits into three subbands 3d0, 3d1, 3d2, which coincide at k = 0, and the 3p band splits into two subbands 3p0 and 3p1.

At m = 0, a maximum of two electrons can be present in the subband, and at $m \neq 0$, the maximum is four electrons. To find the potential it is necessary to know the wave functions of all the electrons, including the internal ones, for which it is possible to neglect the broad band, since it is very small, Hartree[15] already called attention to the low sensitivity of the internal electronic layers of the atom to perturbations of the potential in the process of successive approximations. The situation is similar in a crystal. Therefore the wave functions of the internal electrons and their contributions to the potentials are calculated only once (for the initial approximation) and are not changed in the subsequent process. Special calculations have fully confirmed the validity of this statement.

To determine the dependence of the pressure on the density in solids, one usually first calculates the energy of the body, and then its change following the change of the configuration of the body (for example, of the distances between nuclei). This method calls for knowledge of the energy of the body for two closed configurations. Since the change of the energy of the body is negligible compared with the absolute value of the energy even at large compressions, such a method of calculating the pressure calls for a very high energy-calculation accuracy. Our purpose therefore is to obtain a direct formula for the pressure in solids. The expressions for the force acting on the nucleus, in the form of an integral over the wave functions of the configuration in question, was obtained by Feynman[16] for the case of molecules.

It turns out that for solids it is also possible to obtain an expression for the pressure in terms of the wave functions of the system in the state under consideration. The expression so obtained contains an integral over the surface of the unit cell of the crystal (kinetic pressure) and the Coulomb (mainly exchange-correlation) interaction between the electrons in different cells (exchange pressure), while the Coulomb interaction within one cell is excluded[17,18].

Calculation of the exchange part of the pressure directly from the wave functions is a very complicated matter. In the case of large compressions, the formula obtained for the exchange pressure goes over into the well known formula for the free electron gas. Therefore, as a rule, we shall henceforth, use for estimates of the exchange pressure the free-electron-gas approximation

$$p_{ex} = -e^2W^2/3\pi^3a_0^4;$$

here a_0 is the Bohr radius and W the difference between the Fermi energy and the potential on the boundary of the cell. This means that we assume all the electrons having an energy higher than the potential on the edge of the cell to be almost free.

In all the calculations considered by us, the wave functions were obtained in the Hartree approximation. Recently, V. G. Podval'nyĭ obtained the wave functions for iron by taking into account the exchange interaction of the electrons in one cell, which apparently constitutes the principal part of the exchange interaction of the electrons. Such a formulation of the problem has made it possible to obtain an integro-differential equation for the radial function, which, as before, does not depend on the vector k. Because of this circumstance, the general scheme for calculating the energy bands remained the same as before (we recall that the boundary conditions depend on k). We note that in the calculation of the radial density matrix no account was taken of the dependence of the radial functions on the quasimomentum. As shown by a special experiment, this limitation is not very important. The potential was chosen to be the Hartree self-consistent potential. We present the main results. The configuration of the E(k) curves was in the main retained, and the width of the bands changed slightly (for example, for 3d0 at $\delta = 2$ the width is 0.787 in place of 0.082 according to Hartree)*. In Table I we give the values of p_{kin} (in 10^6 atm) in the Hartree-Fock (HF) approximation (under the indicated limitations), and p_{kin} calculated in the Hartree (H) approximation. We see, as expected, that the relative contribution of the exchange decreases strongly with increasing compression.

Table I

δ	p_{kin} (H)	p_{kin} (HF)	p_{kin} (H)/p_{kin} (HF)
0.746	0.239	0.103	2.320
1.073	1.836	1.541	1.191
2.005	10.278	9.459	1.086
4.000	53.613	50.896	1.053

It should be noted that the computation time (even without self-consistency) is increased by approximately seven times compared with the calculation in the Hartree approximation.

Thus, the results of this investigation confirm fully the advantages of using the Hartree approximation in calculating the wave functions.

So far we have considered only the temperature T = 0. At higher temperatures, the thermal energy and the thermal motion of the electrons become significant, especially in the reduction of data on the dynamic compressibility of metals by shock waves. With the aid of the quantum-mechanical theory that takes into account the character of the occupation of the concrete bands, it was possible to uncover interesting singularities in the course of the thermal energy and the thermal pressure as functions of the density and of the temperature, something that could not be observed within the framework of the statistical theory. With the aid of the apparatus of the quantum field theory, an equation of the Hartree-Fock type was obtained for nonzero temperatures. Knowledge of the eigenvalues of this equation suffices for the calculation of the thermal energy, the thermal pressure, and the associated Gruneisen coefficient of the electrons γ_e. At temperatures $T < 10^5$°K it is possible to use as the eigenvalues the values of the band energies obtained at T = 0.

We now proceed to a brief description of the most interesting results for different metals. We note first that within the framework of the described method it is possible to obtain accurately the different compressibilities and the normal densities of elements whose atomic numbers differ by unity, for example titanium and vanadium, nickel and copper. The main peculiarities of lead, namely the large compressibility and the small normal density (11.4 g/cm^3) compared with other metals with large Z, are well described by the theory. This is explained by the fact that in lead there are only two electrons in the 6d band. With Dy and Nd as examples, a sharp change in the character of the compressibility with increasing density was observed; this change is characteristic of many rare-earth elements. Recently this was also demonstrated experimentally[19-21].

Allowance for the individual peculiarities of the

*In this review we use atomic units: the length unit is the Bohr radius $a_0 = \hbar^2/me^2$, and the energy unit is $e^2/a_0 = 27.23$ eV.

filling of the energy bands makes it possible to reveal irregularities in the cold-pressure curve and phase transitions of the electronic type. If the irregularity on the pressure curve has a nonmonotonic character (of the Van-der-Waals type), this means that a jump of the density occurs here (first-order phase transition). One of the most pronounced examples of a phase transition connected with electronic realignment upon compression is the density jump in potassium. It appears theoretically at a pressure of 0.18 million atmospheres. The possibility of such a phase transition in alkali metals was considered qualitatively by Arkhipov[22]. Alekseev[23] obtained by calculation a phase transition with a density jump in K, Rb, and Cs, the calculated transition pressure for Rb and Cs being close to the experimental one. In calcium, just as in potassium, a transition of the electrons from the 4s band to the 3d band was observed upon compression, leading to the appearance of a plateau on the cold-pressure curve (see Fig. 21 below). However, apparently because of the inaccuracy of the method, the intersection of the 4s and 3d bands was obtained at $\delta = 1.4$. Thus, the metallic properties of calcium at normal density ($\delta = 1$) are not represented by us quite accurately. The rare case of tangency of completely filled and unfilled bands within the 3d band was observed in solid argon compressed by a factor of more than 2.5[28]. At lower degrees of compression, the solid argon is a dielectric and the six external electrons are in the 3p band. It was recently revealed experimentally that the shock adiabat of vanadium has a noticeable kink, whereas the shock adiabat of the neighboring element titanium has no kink[20,24]. Our results are in reasonable agreement with this fact.

A very interesting electron realignment is observed in aluminum. It consists of a change in the direction of the 3d0 subband upon compression, causing a bend to appear on the cold-pressure curve. The thermal energy of the electrons is represented in the form $E_T = \varphi T^2/2$, and the thermal pressure in the form $p_T = \gamma_e E_T \rho$ (here φ is the coefficient of the electronic specific heat and γ_e is the Gruneisen coefficient). It is well known that $\varphi(\delta)$ is proportional to the density of the electronic states on the Fermi surface, and γ_e is connected with the rate of change of $\varphi(\delta)$. It is obvious that φ and γ_e depend very strongly on the structure of the electron bands. Therefore the developed theory and the calculations based on it explain both the anomalously large values of the electronic specific heat of transition metals, and also the very large difference (by a factor of 12 times) between the specific heats of nickel and copper at low temperatures. In some cases, the density of the electron levels increases upon compression, leading also to negative values of γ_e. This interesting phenomenon was observed in Al and K. The dependences of φ and γ_e on the density and on the temperature, observed by us, are in good agreement with the experimental data, for example, for Ni and Fe[25].

In conclusion we wish to mention the predicted changeover of nickel into a dielectric at a relative compression $\delta = 5$ and a pressure of 120 million atmospheres[29]. The cause of this phenomenon is that the nickel atom has 28 electrons, i.e., precisely the number of electrons that would be filled by levels with $n \leq 3$ if their arrangement would not differ from the hydrogen-like arrangement.

Actually, the 4s band in metallic nickel under normal conditions lies below the 3d band, and the 3d band is therefore not filled. With increasing density, as we shall show, the 4s band rises rapidly, leading near $\delta = 5$ to a situation wherein all the bands with $n \leq 3$ are filled, and nickel can become a dielectric. It should be noted that this phenomenon vanishes at $\delta > 15$, since an overlap of the 3p and 4d bands takes place.

The calculations presented in this review were performed over six years with electronic computers. The description of many questions touched upon here can be found in Gandel'man's dissertation[26]. Some results of the calculations were published earlier, namely the data on iron, aluminum, and potassium[27] and on solid argon[28].

We are very grateful to Academician Ya. B. Zel'dovich for great interest in the work during all its stages, and also to L. V. Al'tshuler, N. A. Dmitriev for a discussion.

2. Hartree Self-consistent Field in a Crystal

As already noted in Sec. 1, the complete Hartree problem in a crystal reduces to a solution of an equation with Bloch's periodic boundary conditions in one cell. In this case the equation takes the form

$$\left(-\frac{1}{2}\Delta_x - Z\sum_{\mathbf{l}}|\mathbf{x}-\mathbf{l}|^{-1} - E_i\right)\psi_i(\mathbf{x}) + \left(\sum_j \int |\psi_j(\mathbf{y})|^2 |\mathbf{x}-\mathbf{y}|^{-1} d|\mathbf{y}|\right)\psi_i(\mathbf{x}) = 0; \quad (1)$$

Here $\psi_i(\mathbf{x})$ is the one-electron wave function; the integration is carried out over the cell under consideration. By the quantum-state number i is meant the aggregate $\{\bar{n}, m, \mathbf{k}\}$. The quantum numbers n and m were defined in Sec. 1, n denoting for brevity the set nl_0.

Inside the cell, the solution of Eq. (1) will be sought in the form of an expansion in spherical harmonics (eight harmonics are used)*:

$$\psi_{\mathbf{k}\bar{n}m}(\mathbf{x}) = \sum_{l=m}^{7} i^l A_{\bar{n}ml}(k)\, f_l[E_{\bar{n}m}(k); r]\, Y_{lm}^{\mathbf{k}^0}(\theta, \varphi). \quad (2)$$

The polar axis for the spherical harmonics is chosen to be the direction of $\mathbf{k}$ ($\mathbf{k}^0$ is the unit vector of this direction); r, θ, and φ are the spherical coordinates of $\mathbf{x}$.

To obtain the equation for the radial function $f_l(r)$, we substitute (2) in (1), multiply the equation by $i^{-l} Y^*_{lm}(\theta, \varphi)$, and integrate over the angle variables θ and φ. After simple transformations we obtain an equation for the function $f_l(r)$

$$\frac{1}{2r^2}\frac{d}{dr}\left(r^2\frac{df_l}{dr}\right) + \left[E_{\bar{n}m}(k) - V(r) - \frac{l(l+1)}{2r^2}\right] f_l(r) = 0, \quad (3)$$

where

$$V(r) = -\frac{Z}{r} + \sum_{\bar{n}', m'} \varepsilon_{m'} \sum_{l'=m'}^{7} \int \frac{6k'^2\, dk'}{k_0^3} A^2_{\bar{n}'m'l'}(k') \int_0^{r_0} U_0(r, r') f^2_{l'}(r') r'^2\, dr',$$

$$U_0(r, r') = \begin{cases} 1/r' & \text{if } r < r', \\ 1/r, & \text{if } r > r', \end{cases} \qquad \varepsilon_m = \begin{cases} 1, & m = 0, \\ 2, & m \neq 0. \end{cases} \quad (4)$$

It must be borne in mind that we are considering throughout the case of compensated spins, so that

*E. S. Pavlovskiĭ and V. A. Tarasov (private communication) have shown by calculation that eight harmonics suffice in the case when there is no potential ("the empty-cell test").

formula (4) includes the factor 2 as a result of summation over the spins. By k we always mean the dimensionless quantity kr_0, where r_0 is the cell radius. Integration with respect to k is carried out over all the filled states, i.e., those lying below the Fermi surface. Starting from the fact that the volume of the unit cell in k-space is equal to $(2\pi)^3(4\pi r_0^3/3)^{-1}$, we readily obtain the maximum possible value $k_0 = (9\pi/2)^{1/3} = 2.418$.

The function $f_l(r)$ is best normalized as follows: $\int_0^{r_0} f_l^2(r)r^2dr = 1$. To satisfy the normalization condition of the function $\psi_{k\bar{n}m}$, it is necessary to satisfy the condition $\sum_{l=m}^{7} A^2_{\bar{n}ml}(k) = 1$.

The coefficients A(k) can be found by using the boundary conditions. In the Wigner-Seitz approximation, Bloch's boundary conditions connect the values of the function and its derivative at diametrically opposite points of the sphere $r = r_0$:

$$\left.\begin{aligned} &\psi(r_0, \theta, \varphi)\, e^{-ik\cos\theta} = \psi(r_0, \pi-\theta, \pi+\varphi)\, e^{ik\cos\theta}, \\ &e^{-ik\cos\theta}\frac{\partial\psi}{\partial r}\Big|_{r_0,\theta,\varphi} = -e^{ik\cos\theta}\frac{\partial\psi}{\partial r}\Big|_{r_0,\pi-\theta,\pi+\varphi}. \end{aligned}\right\} \quad (5)$$

Substituting the expansion (2), multiplying (5) by $i^{-l}Y^*_{lm}(\theta, \varphi)$, and integrating over the angle variables, we get

$$\left.\begin{aligned} &\sum_{l'=m}^{7} A_{\bar{n}ml'}(k)\, a_{ll'm}(k)\, f_{l'}(r_0) = 0, \quad \text{if } l \text{ is odd}, \\ &\sum_{l'=m}^{7} A_{\bar{n}ml'}(k)\, a_{ll'm}(k)\, \frac{df_{l'}}{dr}\Big|_{r=r_0} = 0, \quad \text{if } l \text{ is even}. \end{aligned}\right\} \quad (6)$$

where the coefficients are

$$a_{ll'm}(k) = i^{l'-l}\int Y^*_{lm}Y_{l'm}e^{-ik\cos\theta}\,d\Omega.$$

With the aid of the expansion of a plane wave in spherical harmonics and Gaunt's formula we can calculate all these coefficients.

The system (6) has nontrivial solutions if the determinant of the system differs from zero. Solving Eq. (3), we compile beforehand a table of values of the function $f_l(r)$ and of its derivative on the boundary of the cell for trial values of E. Since $a_{ll'm}$ are functions of k, the determinant of the system (6) is a function of E and k. The vanishing of the determinant yields the sought connection between the energy and the quasimomentum ($E_{nl_0m}(k)$).

To calculate the potential V(r) [Eq. (4)] it is necessary to know the radial functions of both the outer and the inner electrons. The use of the computation scheme described by us is not suitable for the radial functions of the inner electrons, since these functions are localized near the nucleus. Consequently, starting with a certain point, the true values of the function become negligibly small, and as a result of the inaccurate knowledge of the eigenvalue and of the inevitable errors in the numerical calculations we find ourselves with an exponentially growing solution. To find the eigenvalues and the functions $f_l(r)$ of the internal electrons, we use a procedure based on an exact solution of Eq. (3) jointly with the use of the quasiclassical approximation. The energy eigenvalue is obtained from the condition for the smoothness of the joining of the two pieces of the curve.

By way of the initial approximation for the potential, at sufficiently large degrees of compression, it is natural to choose the Thomas-Fermi potential of the compressed atom at T = 0. It is not advantageous to confine oneself to only the initial approximation, since this leads to an appreciable deviation from the exact solution of the problem. For example, calculations show that in Dy at $\delta = 2$ we have $p_{kin} = 0.719$ for the last approximation and $p_{kin} = 2.92$ for the initial approximation, and at $\delta = 4$ we have $p_{kin} = 7.52$ as against 13.85.

Even in those cases when the Thomas-Fermi potential is a good approximation to the "self-consistent" potential, the iteration process diverges as a rule (we have already noted this circumstance in Sec. 1). Particularly large difficulties arise when $\delta \sim 1$, and the statistical potential becomes a poor initial approximation, and furthermore there exist additional factors contributing to the divergence (for example, the instability of the d-band in the approximation process*). The difficulties arising in this case have led to two mathematical problems:

a) how to change the calculation procedure to make the successive-approximation process convergent;

b) how to find an improved initial approximation.

Thus, in essence, we deal with the solution of the equation

$$\varphi_\delta(x) = A_\delta\varphi_\delta(x), \quad (7)$$

where A_δ is a nonlinear operator describing the aggregate of the actions described above, x is the spatial variable, φ_δ is a potential, and δ is the relative density.

In our calculations of the potential of the self-consistent field we employ the following procedure. With the aid of the initial (zeroth) approximation φ^0 we obtain the energy bands and a new approximation φ^1. Specifying δ^1, we find φ^2. We seek a new approximation in the form $\varphi^3 = \beta\varphi^1 + (1-\beta)\varphi^0$, where the number β is determined from the formula

$$\beta = -\int \Delta\varphi^0(\Delta\varphi^1 - \Delta\varphi^0)\,x^2\,dx \Big/ \int (\Delta\varphi^1 - \Delta\varphi^0)^2\,x^2\,dx, \quad \Delta\varphi^n = \varphi^{n+1} - \varphi^n.$$

Using the φ^3 obtained in this manner, we find φ^4 and $\varphi^5 = \beta\varphi^4 + (1-\beta)\varphi^3$, etc. The number β remains unchanged in the process of obtaining the new approximations.†

Let us assume that the initial approximation φ^0 is sufficiently close to the solution; then the operator in (1) can be linearized:

$$A\varphi = A\varphi^0 + A_\pi(\varphi - \varphi^0).$$

Apparently, even such an approximation gives an idea of the general character of the iteration process. In this case we would deal with a linear inhomogeneous equation. It can be shown that in the linear case the method employed by us is one of the variants of the gradient method.

*Thus, filling of 5d takes place for Dy in the zeroth approximation, whereas in the first approximation 4f becomes filled.

†Experiment has shown that in the case of poor convergence or divergence of this process, attempts to recalculate β do not improve the situation.

Calculations with the aid of the described procedure were carried out for many elements (Fe, Al, K, Pb, etc.) at different degrees of compression. To obtain satisfactory results it suffices, as a rule, to use 3–5 computing approximations. The number of approximations increases at $\delta \sim 1$. In these cases, the β-process frequently even diverges. The other method employed by us consists essentially of constructing a new approximation from one obtained with the aid of two numbers determined from the condition that the error be minimized. Particularly useful is a procedure in which the new approximation is sought in the form $\overline{\varphi} = \varphi^n + \gamma(\varphi^m - \varphi^n)$, where

$$\gamma = -\int \Delta\varphi^n (\Delta\varphi^m - \Delta\varphi^n) x^2 dx \Big/ \int (\Delta\varphi^m - \Delta\varphi^n)^2 x^2 dx.$$

This procedure makes it possible to use approximations obtained during different stages of the process. The convergence of the successive-approximation process can be determined by the condition $m_n \ll m_0$, where $m_0 = \int (\Delta\varphi^n)^2 x^2 dx$. If a solution has already been obtained for some degree of compression δ, an improved initial approximation in the vicinity of δ can be constructed using the Thomas-Fermi potential and the known solution, by making use of the fact that the ratio of the functions changes in this vicinity less strongly than the functions themselves.

3. Derivation of the Formula for the Pressure at T = 0. Thermal Energy and Thermal Pressure of the Electrons

We use the general quantum-mechanical formula for the derivative of the current with respect to time[30] (all the quantities are regarded as functions of the time and of the coordinates of all the particles—both nuclei and electrons):

$$\left.\begin{aligned} m_\alpha \frac{\partial j_{\alpha\mu}}{\partial t} &= -\sum_{\lambda,\nu} \frac{\partial T_{\alpha\mu,\lambda\nu}}{\partial q_{\lambda\nu}} - \Psi\Psi^* \frac{\partial U}{\partial q_{\alpha\mu}}, \\ T_{\alpha\mu,\lambda\nu} &= \\ &= -\frac{1}{4m_\lambda}\left(-\Psi^* \frac{\partial^2\Psi}{\partial q_{\lambda\nu}\partial q_{\alpha\mu}} - \Psi \frac{\partial^2\Psi^*}{\partial q_{\lambda\nu}\partial q_{\alpha\mu}} + \frac{\partial\Psi}{\partial q_{\alpha\mu}}\frac{\partial\Psi^*}{\partial q_{\lambda\nu}} + \frac{\partial\Psi}{\partial q_{\lambda\nu}}\frac{\partial\Psi^*}{\partial q_{\alpha\mu}}\right); \end{aligned}\right\} \quad (8)$$

where $q_{\alpha\mu}$ denote the μ-th coordinate of the particle α, and $\Psi(t, q)$ is the wave function of the system of particles.

We integrate Eq. (8), taken for the μ-th coordinate of the n-th particle over the configuration space of all the remaining particles:

$$m_n \frac{\partial}{\partial t}\int j_{n\mu} d\tau_n = -\sum_{\lambda,\nu}\int \frac{\partial T_{n\mu,\lambda\nu}}{\partial q_{\lambda\nu}} d\tau_n - \int \frac{\partial U}{\partial q_{n\mu}} \Psi^*\Psi\, d\tau_n; \quad (9)$$

here

$$U = \frac{1}{2}\sum_{i\neq j} \frac{Z_i Z_j}{r_{ij}}, \quad \frac{\partial U}{\partial q_{n\mu}} = \sum_{j\neq n} Z_n Z_j \frac{\partial}{\partial q_{n\mu}}\left(\frac{1}{r_{nj}}\right).$$

The first integral in the right side vanishes if the index λ does not pertain to the n-th particle. On the left side is the μ-th projection of the force density f_n acting on the n-th particle.

We introduce the notation

$$\int |\Psi|^2 d\tau_{nm} = \Gamma_{nm}(q, q'),$$

where $d\tau_{nm}$ is an element of configuration space without the coordinates of two particles. After summing (9) over n, we obtain an expression for the total force density:

$$f_\mu = -\sum_\nu \frac{\partial T_{\mu\nu}(q)}{\partial q_\nu} - \sum_{n,j} Z_n Z_j \int_\Omega \Gamma_{nj}(q, q') \frac{\partial}{\partial q_\mu}\frac{1}{|q-q'|} dq',$$

where

$$T_{\mu\nu}(q) = \sum_n \left[\int T_{n\mu,n\nu} d\tau_n\right]_{q_n = q},$$

and Ω is the volume of the entire space.

Let us find the force acting on a certain selected volume ω (for example, the unit cell of the crystal):

$$F_\mu = \int_\omega f_\mu(q)\, dq = \quad (10)$$

$$= -\oint_\omega \sum_\nu T_{\mu\nu}(q) n_\nu\, ds - \sum_{n,j} Z_n Z_j \int_\omega dq \int_\Omega dq' \Gamma_{nj}(q, q') \frac{\partial}{\partial q_\mu}\frac{1}{|q-q'|};$$

$\{n_\nu\}$ is the normal to the surface of the cell, $\Gamma_{nj}(q, q')$ is the probability that the n-th particle is at the point q and the j-th particle at the point q′. $\gamma_n(q) = \int |\Psi|^2 d\tau_n$ is the probability that the n-th particle is at the point q. The difference

$$\Gamma_{nj}(q, q') - \gamma_n(q)\gamma_j(q') = -\Gamma_{nj}(q, q')$$

describes the exchange phenomenon. The density of the electric charge is $\rho(q) = \sum_n Z_n \gamma_n(q)$.

We now break up the integral $\int dq'$ in (10) into two parts:

$$\int_\omega dq' \text{ and } \int_{\Omega-\omega} dq'.$$

The first part yields zero, since when q is replaced by q′ and vice versa the integral equation reverses sign. Although the total force F_μ is equal to zero, we can separate from (10) the force $F_\mu^{(gh)}$ exerted on a given cell g by any other cell h, and also the surface forces. It is precisely in terms of these two quantities that we shall express the pressure henceforth. It is convenient to separate the second term in the right side of formula (10) into two terms:

$$\sum_{n,j}^{n\neq j} Z_n Z_j \int_\omega dq \int_{\Omega-\omega} dq' \Gamma_{nj}(q, q') \frac{\partial}{\partial q_\mu}\frac{1}{|q-q'|}$$

$$= \int_\omega \rho(q)\, dq \int_{\Omega-\omega} \rho(q')\, dq' \frac{\partial}{\partial q_\mu}\frac{1}{|q-q'|}$$

$$- \int_\omega dq \int_{\Omega-\omega} dq' \frac{\partial}{\partial q_\mu}\frac{1}{|q-q'|} \sum_{n,j} Z_n Z_j \{\Gamma_{nj}(q, q') + \delta_{nj}\gamma_n(q)\gamma_n(q')\}. \quad (11)$$

We now use the fact that the nuclei can be regarded as immobile. The terms due to the nuclei in the tensor $T_{\mu\nu}(q)$ vanish, and we are left only with the contribution from the interaction of the nuclei in electrostatic term of (11). However, for electrically neutral cells with sufficiently good symmetry, this entire term can be neglected, as already mentioned in Sec. 1. Thus, only the electron terms remain in the expression for the force F_μ.

We introduce the following convenient notation: N is the total number of electrons

$$\rho(q) = \sum_n \gamma_n^e(q) = N\int |\Psi(q_1, q_2, \ldots, q_N)|^2 d\tau_2 \ldots d\tau_N,$$

$$\Gamma(q, q') = \sum_{n,j} \Gamma_{nj}^e(q, q') = N(N-1)\int |\Psi(q, q', q_3, \ldots, q_N)|^2 d\tau_3 \ldots d\tau_N,$$

$$\rho(q, q') = N\int \Psi^*(q', q_2, \ldots, q_N)\Psi(q, q_2, \ldots, q_N) d\tau_2 \ldots d\tau_N.$$

In these equations we used the asymmetry of the wave

function $\Psi(q_1, q_2, \ldots, q_N)$. The stress tensor $T_{\mu\nu}(q)$ is expressed in terms of the density matrix in the form

$$T_{\mu\nu}(q) = \frac{1}{4}\left[-\frac{\partial^2\rho(q', q)}{\partial q_\mu \partial q_\nu} - \frac{\partial^2\rho(q', q)}{\partial q'_\mu \partial q'_\nu} + \frac{\partial^2\rho(q', q)}{\partial q'_\mu \partial q_\nu} + \frac{\partial^2\rho(q', q)}{\partial q_\mu \partial q'_\nu}\right]_{q'=q}. \quad (12)$$

Substituting (11) and (10) and omitting the first term, we obtain the force acting on the g-th cell

$$F_\mu^{(g)} = -\int_{\omega_g} \sum_\nu T_{\mu\nu}(q)\, n_\nu\, ds + \sum_{h\neq g} F_\mu^{(gh)}, \quad (13)$$

$$F_\mu^{(gh)} = -\int_{\omega_g} dq \int_{\omega_h} dq' \{\Gamma(q, q') - \rho(q)\rho(q')\} \frac{\partial}{\partial q_\mu} \frac{1}{|q-q'|}. \quad (14)$$

To calculate the pressure it is necessary to find the work done by the forces between cells in the case of uniform expansion of the body in all directions in a ratio $1 + \alpha$. The obtained change of the system energy δE must be divided by the change of the volume $\delta V = 3\alpha\omega$ per cell, multiplied by the number of cells, and the sign of the quotient must be reversed. The work of the surface force is equal to the average value of $T_{\mu\nu}(q)$ on the surface of the cell, multiplied by the change in volume. The contribution made by this force to the pressure will be called the kinetic pressure and denoted

$$p_{\text{kin}} = \int p_{\text{kin}}(q) \frac{d\Omega}{4\pi}, \quad (15)$$

$$p_{\text{kin}}(q) = \sum_{\mu,\nu} T_{\mu\nu}(q)\, n_\mu n_\nu = \frac{1}{4}\left[-\frac{\partial^2\rho(q, q')}{\partial n^2} - \frac{\partial^2\rho(q, q')}{\partial n'^2} + 2\frac{\partial^2\rho(q, q')}{\partial n\, \partial n'}\right]_{q=q'}. \quad (16)$$

The work of the Coulomb forces $F_\mu^{(gh)}$ is written in the form

$$\alpha \sum_{g,h} F^{(gh)} R_{gh}/2,$$

where R_{gh} is the distance between the centers of the g-th and h-th cells. The contribution made by these forces to the pressure will be called the exchange pressure and denoted

$$p_{\text{ex}} = -(1/6\omega) \sum_{h\neq 0} F^{(0,h)} R_{0,h}. \quad (17)$$

The index zero denotes the cell under consideration. Thus, the total pressure is

$$p = p_{\text{kin}} + p_{\text{ex}}. \quad (18)$$

The derivation presented here was first published in a paper by Gandel'man[18]. In a paper by Dmitriev[17], the result obtained here for pressure was derived in another way: perturbation theory was used to calculate directly the small change of energy resulting from a small change in the volume. We shall be interested in the future in the particular case when the wave function of the system is represented in the form of a determinant of single-electron functions $\psi_i(q)$. In this case it is easy to obtain the well known formulas

$$\rho(q, q') = \sum_{i=1}^{N} \psi_i^*(q')\psi_i(q), \quad \rho(q) = \sum_{i=1}^{N} |\psi_i(q)|^2,$$
$$\Gamma(q, q') - \rho(q)\rho(q') = -|\rho^+(q, q')|^2 - |\rho^-(q, q')|^2;$$

Here ρ^+ is the part of the density matrix for electrons with one direction of the spin, ρ^- is for electrons with opposite spin direction. Then the formula for $p_{\text{kin}}(q)$ takes the form

$$p_{\text{kin}}(q) = \frac{1}{4}\sum_i \left[-\psi_i^*(q)\frac{\partial^2\psi_i(q)}{\partial n^2} - \psi_i(q)\frac{\partial^2\psi_i^*(q)}{\partial n^2} + 2\left|\frac{\partial\psi_i(q)}{\partial n}\right|^2\right]. \quad (19)$$

On the basis of the approximation of spherical cells and using formula (2), we obtain (after averaging over different directions of the quasimomentum) the following formula for the kinetic pressure in atomic units ($e^2/a_0^4 = 2.93 \times 10^8$ atm)*:

$$p_{\text{kin}} = \frac{1}{4\pi}\sum_{\bar{n},m} \varepsilon_m \int \frac{3k^2\, dk}{k_0^3} \sum_{l=m}^{7} A_{\bar{n}ml}(k)\{[f'_{\bar{n}ml}(k, r_0)]^2 - f_{\bar{n}ml}(k, r_0) f''_{\bar{n}ml}(k, r_0)\},$$
$$E_{\bar{n}m}(k) \leqslant E_F. \quad (20)$$

It is seen from (20) that the contribution of the inner electrons to the kinetic pressure is negligible, since the radial wave functions $f_{\bar{n}ml}(k, r_0)$ on the surface of the cell are very small for these electrons.

We shall now touch upon the question of the thermal energy and thermal pressure of the electrons. The reader interested in details is referred to[18].

The electronic specific heat C_T is expressed in terms of the eigenvalue of the energy $E_i(k)$ as follows:

$$C_T = \sum_i E_i \left(\frac{\partial f_i}{\partial T}\right)_{N,V}, \quad (21)$$

where

$$f_i = [1 + e^{(E_i-\mu)/T}]^{-1}.$$

The chemical potential μ is determined from the normalization condition

$$\sum_i f_i = N, \quad (21')$$

where N is the number of electrons. We recall that summation over i denotes summation over the bands and integration over the quasimomentum.

In our case we get after elementary transformations,

$$C_T = \sum_{\bar{n},m} \varepsilon_m \int_0^{k_0} \frac{6k^2\, dk}{k_0^3} \frac{x_{\bar{n}m}[x_{\bar{n}m} + (d\mu/dT)]}{e^{x_{\bar{n}m}} + e^{-x_{\bar{n}m}} + 2}, \quad (22)$$

$$\frac{d\mu}{dT} = -\frac{\sum_{\bar{n},m} \varepsilon_m \int_0^{k_0} \frac{k^2 x_{\bar{n}m}\, dk}{e^{x_{\bar{n}m}} + e^{-x_{\bar{n}m}} + 2}}{\sum_{\bar{n},m} \varepsilon_m \int_0^{k_0} \frac{k^2\, dk}{e^{x_{\bar{n}m}} + e^{-x_{\bar{n}m}} + 2}}; \quad (23)$$

here $x_{\bar{n}m} = [E_{\bar{n}m}(k) - \mu]/T$. The condition for the calculation of μ is

$$\sum_{\bar{n},m} \varepsilon_m \int_0^{k_0} \frac{6k^2\, dk}{k_0^3} \frac{1}{1 + e^{x_{\bar{n}m}}} = Z.$$

Knowledge of the specific heat enables us to find the thermal energy

$$E_T = \int_0^T C_T\, dT$$

and the thermal pressure

Table II. Occupation numbers of electrons in the states n_l

δ=1.01		δ=2,44			
l	3d0	l	3d0	3d1	3d2
0	0.650	0	0.303	—	—
1	0.235	1	0.152	0.023	—
2	0.009	2	0.152	0.153	0.091
3	0.077	3	0.088	0.010	0,002

$$n_l = \varepsilon_m \int_{E(k)\leq E_F} \frac{6k^2}{k_0^3} A_l^2(k)\, dk.$$

*The pressure in all the calculations is in units of 10^6 atm.

$$p_T = T\int_0^T \frac{1}{T^2}\left(\frac{\partial E_T}{\partial V}\right)_T dT.$$

Using the definition of φ and γ_e (see Sec. 1), we can obtain the simple formula

$$\gamma_e = -\frac{\partial \ln \bar{\varphi}}{\partial \ln \delta}\frac{\bar{\varphi}}{\varphi}, \quad (24)$$

where $\bar{\varphi} = (1/T)\int_0^T \varphi\, dT$. At low temperatures $\bar{\varphi} \approx \varphi$ and $\gamma_e = -\partial \ln \varphi / \partial \ln \delta$.

II. RESULTS OF INVESTIGATIONS OF THE PROPERTIES OF CERTAIN METALS AT HIGH PRESSURES AND TEMPERATURES

The theory developed in Ch. I served as the basis of the calculations which we shall now analyze.

1. Aluminum

Since aluminum exhibits very unusual properties upon compression, the calculations for it were performed in particular detail: δ = 0.658, 1.01, 1.01, 1.48, 1.96, 2.44, 2.95, 3.5, 4.18, 5.5, and 7.

In the aluminum atom we have the configuration $1s^2 2s^2 2p^6 3s^2 3p$, and the 3d level lies 0.148 atomic units above the 3p level[2]. In aluminum metal, however, the outer electron is in the 3d band and not in 3p. To be sure, the 3d0 subband, in which the outer electron is located, is directed downward and at large k the wave function of the electron contains a large admixture of s and p states. This fact is demonstrated in Table II. At normal density (ρ_0 = 2.7 g/cm^3), the outer electron is located in the 3d0 subband, with k_I = 1.919, so that the 3d0 band is half-filled. A characteristic feature is that upon compression the width of the subband 3d0 decreases, while the subbands 3d1 and 3d2 broaden. At δ = 1.01, the distance from the Fermi energy E_F to the edge of 3d0 is 0.033 atomic units, at δ = 1.48 this distance amounts to only 0.018 atomic units, and at δ = 1.96 only 0.003 atomic units.

We observe here a very curious electron realignment, consisting of the rotation of the direction of 3d0 upon compression. It is seen from Fig. 1 that E_F already intersects all three subbands of 3d simultaneously at δ = 2.44, and 3d0 is even intersected three times. With further compression, E_F already intersects immediately all three subbands of 3d, and their width increases with increasing compression. This peculiar realignment of the bands is of very great importance for the explanation of the properties of the Gruneisen coefficient of the electrons in aluminum, as will be shown later.

Figure 2 shows the cold-pressure curve p(δ). At normal density, there is an error of about 0.5 million atm in the pressure, and holds up to compressions $\delta \sim 2.5$. Beyond this, the calculated pressures are higher than those obtained by the TFC method. For example, at δ = 5.5, the statistical value is 25.7 million atm as against 35.6 million atm in accordance with our calculation. At δ = 10 the pressure curves coalesce completely.

As seen from Table III, at first the contribution of 3s and 3d to the pressure are approximately the same, and with increasing density the contribution of the filled 3s band is much more significant.

On the cold-pressure curve one can see clearly the bend in the region $\delta \sim 2$, connected with the electronic realignment described above. Proceeding to the thermal properties of Al, it should be noted that here $\varphi/2$ depends little on the temperature in almost the entire compression region, with the exception of the realignment region, where the structure of the 3d0 band changes strongly. This occurs in the region $\delta \approx 2-3$. At low temperatures and at normal density, the calculated value is $\varphi/2$ = 26.58, which yields φ = 518 erg/g-deg^2.* This agrees well with the experimental value 500 erg/g-deg^2.

The density of the electronic states on the Fermi surface first increases (at small δ), reaches a maximum at $\delta \approx 2.4$, and then it begins to decrease when the subbands of 3d go simultaneously upward and their width increases with increasing δ. This leads to the appearance of a region of negative γ_e at $1 < \delta < 2.4$,

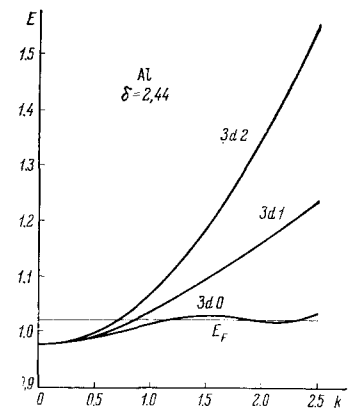

FIG. 1

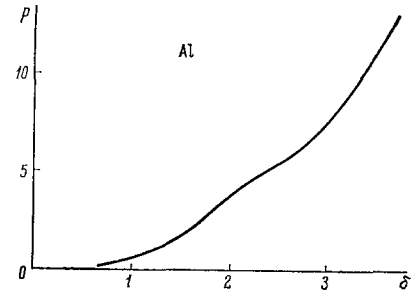

FIG. 2

Table III. Contributions to the kinetic pressure from different bands in Al

δ	2p	3s	3d	δ	2p	3s	3d
1.01	−0.012	0.376	0.700	2.95	−0.522	7.980	4.455
1.48	−0.062	1.278	1.648	3.50	−0.713	12.01	5.88
1.96	−0.168	2.825	3.005	5.50	−0.293	35.25	12.98
2.44	−0.317	4.905	3.930	7.00	+1.782	58.20	19.11

*To obtain φ in the cgs esu system it is necessary to multiple our value of $\varphi/2$ by 9.4 × 56/A.

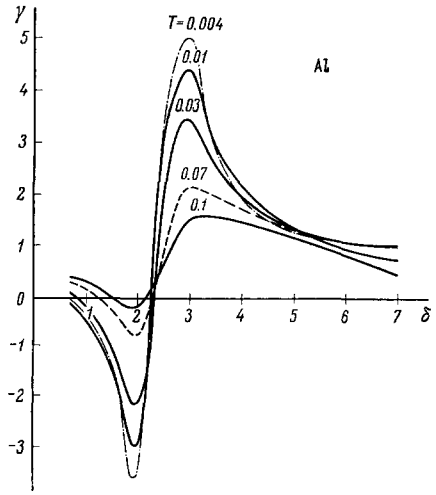

FIG. 3

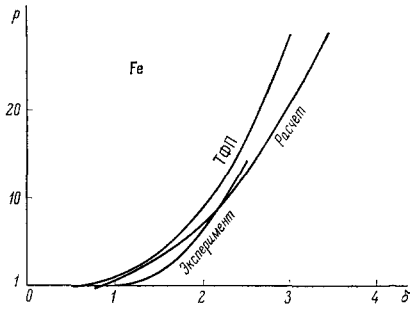

FIG. 4

to the passage of γ_e through zero, and to a rapid growth of γ_e in the region of positive values (Fig. 3).

The presence of a region of negative γ_e and of an inflection in the cold-pressure curve can lead to a rotation of the shock adiabat of Al to the right at $\delta \approx 2$. As shown by the experimental data published in[31,32], such a rotation of the shock adiabat indeed takes place near $\delta \approx 2$. Subsequently, on going over to the region of large positive values of γ_e, one should expect the rotation of the shock adiabat to the left. Using as an example Al, which always was regarded as a "simple" metal from the point of view of the thermal properties of the electrons, we see that upon compression a characteristic change is observed in the 3d0 band, and ensuing anomalous properties of γ_e. Therefore one cannot speak of Al as a "simple" metal, as would follow within the framework of the statistical theory. We note that the obtained structure at $\delta = 1$ in Al differs little in the spherical approximation from the more exact data of Segall[35].

2. Iron

Let us examine the energy structure of a typical representative of the transition-metal group, iron. The calculations were carried out in the compression range $0.75 \leq \delta \leq 8$ (see[27]). The picture of the electron spectrum for the normal density is as follows: the filled 4s band is located below the 3d band, where 3d2 is completely filled, while 3d0 and 3d1 contain two electrons each. We note that the relative arrangement of the bands 4s and 3d is the same as the arrangement of the corresponding levels in the Fe atom. Upon compression, the energy structure experiences a characteristic change—"departure of the 4s band." In the case of a threefold compression, the 4s band is partly filled and overlaps 3d. The value of the overlap is 0.35 at.un. At $\delta = 4$, the overlap decreases to 0.14, and a negligible fraction of electrons is located in 4s. With further compression, the 3d band drops and becomes completely filled, and the 3p band is partly filled and contains four electrons in place of six. Figure 4 shows the calculated plot of $p(\delta)$, and also the experimental curve of Al'tshuler et al.[6] and the curve

Table IV

T \ δ	0.746	1.073	2.005	3	4	5
0.004	1.434	1.439	0.953	0.572	0.509	0.397
0.007	1.483	1.387	1.018	0.571	0.507	0.395
0.010	1.607	1.369	1.068	0.566	0.497	0.378
0.025	1.810	1.379	1.032	0.550	0.400	0.260
0.040	1.716	1.386	1.004	0.660	0.388	0.192
0.070	1.462	1.282	1.040	0.810	0.605	0.308
0.100	1.278	1.169	1.189	0.923	0.764	0.449

calculated by Kalitkin by the TFC method[5]. The results are closer to the experimental data than the TFC curve.

We note that when $\delta \leq 2$ the contributions of the 4s and 3d bands to the kinetic pressure are approximately equal, and the principal role is played by the contribution of the 3d band. At large compressions ($\delta > 4$) the contribution of 3p also becomes significant. Let us describe briefly the thermal properties of the electrons in Fe. At $\delta = 1$, E_F passes somewhat below the subband 3d3 (0.012 at.un.), which is completely filled. Therefore $\varphi/2$ is smaller at $T < 0.012$ at.un. than at higher temperatures, when the excitation of the subband 3d2 comes into play. Calculation of $\varphi/2$ has shown it to have large absolute values of this quantity, an inherent property of transition metals at low temperatures and at normal density, and also the variation of $\varphi/2$ with temperature, which is characteristic of transition metals. In Table IV is given the value of γ_e in Fe. We deal here with the usual case, when the density of the electronic states on the Fermi surface decreases with increasing density of the material, and consequently γ_e is positive. It is seen from the table that in the region $\delta = 1-2$ and at high temperatures, γ_e in Fe is close to unity, which is in good agreement with the experimental data. γ_e decreases with increasing δ.

3. Nickel and Copper

Nickel has two electrons more than iron. The upper band is also the 3d band. Calculations were performed for degrees of compression δ equal to 0.75, 1, 1.5, 2, 3, and 5. At $\delta = 1$ (Fig. 5), the 4s band and the 3d2 subband are filled. E_f intersects the subband 3d1 at $k_F = 2.25$, which is close to the edge of the subband. This circumstance produces a very large density of the electron states at the point of intersection. The

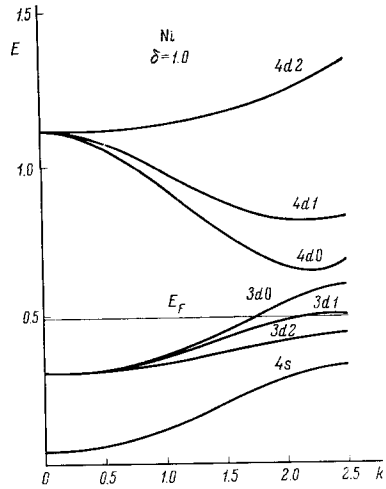

FIG. 5

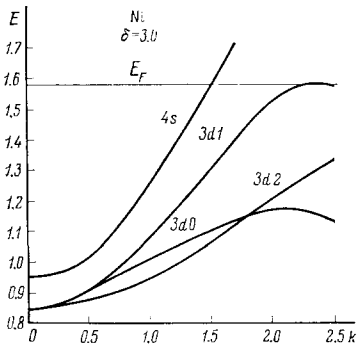

FIG. 6

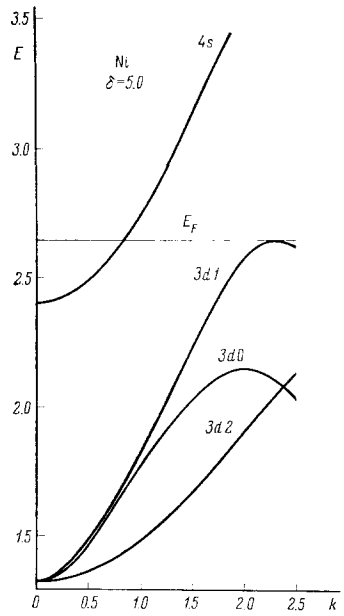

FIG. 7

Table V

T \ δ	δ=0.75	1.0	1.5	2.0	3.0
0.004	2.027	1.470	1.012	0.429	1.256
0.007	1.792	1.484	1.132	0.706	2.714
0.010	1.614	1.504	1.216	0.896	2.723
0.025	1.444	1.446	1.306	1.364	3.629
0.040	1.473	1.408	1.379	1.487	3.604
0.070	1.506	1.295	1.298	1.415	2.947
0.100	1.297	1.185	1.195	1.303	2.280

average number of electrons in the 3d0 and 3d1 subbands is respectively 0.77 and 3.23. At δ = 2, the total width of the 3d band increases strongly (0.73 at.un. as against 0.29 at δ = 1), but the character of the arrangement of the bands remains the same. At δ = 3 (Fig. 6), a realignment of the band takes place. The Fermi surface is inside the 4s band, which contains only 0.5 electrons. Figure 7 shows the picture of the electron bands for δ = 5, demonstrating the start of the transformation of the metal into a dielectric, which was discussed by us in detail in Sec. 1 of Ch. I.

Let us examine now the thermal properties of nickel. Within the framework of our metal, we are able to explain the observed large ratio of the coefficients of the electronic specific heat $\varphi/2$ of nickel and copper. At a temperature 0.002 at.un. (~600°K), this ratio equals 11.4 as against the experimental 11.23. The absolute value $\varphi/2$ for nickel at this temperature is 165.9 in our units, or φ = 1488 erg/g-deg^2. This is also in fair agreement with the experimental value 1240. The large value of $\varphi/2$ at low temperatures in the case of nickel is attributed, just as in the case of other transition metals, to the large density of the electron states on the 3d band near the Fermi surface. In Ni near the Fermi surface in the subband 3d1, the density of states is very large. In Ni, however, $\varphi/2$ decreases strongly with increasing temperature, since all the 3d subbands begin to be excited. A strong temperature dependence of $\varphi/2$ takes place even at higher compressions, since in this case E_F is close to the edge of 3d1. In the region of δ ~ 5, in connection with the transformation into a dielectric, a sharp decrease of $\overline{\varphi}/2$ is observed with increasing density. This exerts a strong influence on the course of the Gruneisen coefficient γ_e, as shown in Table V. We see that γ_e is much larger at δ = 3 than at δ = 2. At δ = 3 the 3d band is almost filled and the opportunities for electron excitation are slight. The value of γ_e at low temperatures and normal density is close to 1.5, and at high temperatures close to 1.0, in reasonable agreement with experiment.

In the Cu atom, the M shell is completely filled and one (outer) electron is located at the 4s level, while the gap between the levels 4s and 3d is equal to 0.23 at.un., whereas in the Fe atom 4s lies 0.13 at.un. below 3d, and the minimal gap between these levels occurs in the Ni atom.* Our calculations have shown, however, that in Fe, Ni, and Cu at normal density the 4s and 3d bands overlap, but the Fermi surface lies inside the 3d band. Nonetheless, calculations at densities below normal give grounds for assuming that on going over to the case of an isolated atom we obtain the just-described arrangement of the levels of these three elements. Indeed, calculation for

*These data are taken from the calculations of Latter [2].

Cu at $\delta = 0.3$ gave a gap with ~0.16, with 4s situated above 3d.

The calculations in Cu were made for $\delta = 0.75$, 1, 1.5, 2, 3, and 5. Figure 8 ($\delta = 1$) shows that the subband 3d0 contains one electron. In this period, the density of the electron states is low. Here we already have a larger admixture of p states. For example, at $k = 2$ we have the following values of the coefficients $A_l(k)$: $A_0 = 0.006$, $A_1 = 0.610$, $A_2 = 0.779$, and $A_3 = 0.081$.

At normal density, the electrons from the 3d and 4s bands are distributed among the states with different orbital angular momenta l in the following manner: $n_0 = 0.70$, $n_1 = 1.03$, $n_2 = 9.09$, and $n_3 = 0.03$.

It is interesting to note that the same arrangement of the 4s and 3d bands as in our spherical approximation was obtained in Segall's calculations[33] for Cu, at normal density, performed by the Green's-function method (Kohn and Rostocker).

The arrangement of the bands in the case of $1 < \delta < 3$ is the same as at $\delta = 1$, but their width is naturally larger. At $\delta = 5$ (Fig. 9), the outer electron is located in 4s.

Figure 10 shows plots of the cold pressure against the density, $p(\rho)$, for Fi, Ni, and Cu. We see that the $p(\rho)$ curve of Cu lies lower than that of Ni. Such an arrangement of the pressure curves agrees with the experimental data, although our values are somewhat higher than the experimental values of the cold pressure in the region $\delta \sim 1$, primarily because of the rather crude estimate of the exchange pressure. The error in the determination of the normal density in Cu is the same as in Ni (~30%) (Table VI).

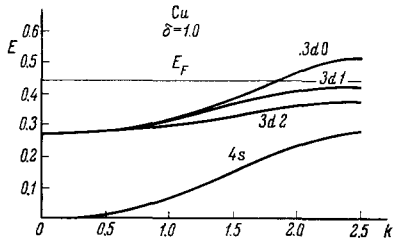

FIG. 8

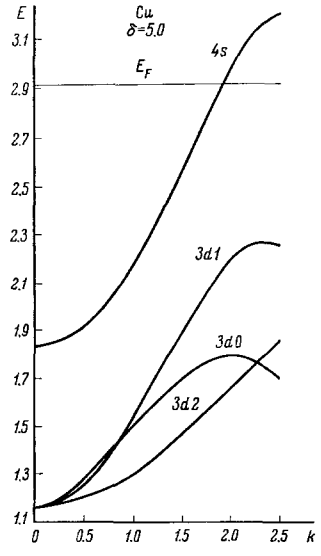

FIG. 9

An investigation of the thermal properties of the electrons in Cu has shown less abrupt changes of $\varphi/2$ than in Ni. At $T = 0.001$ and $\delta = 1$ we have $\varphi = 131$ erg/g-deg^2, which is in good agreement with the experimental value 110 erg/g-deg^2.

At small δ, the $\varphi/2(T)$ curves have a characteristic maximum: $\varphi/2$ increases with increasing excitation of the filled subband of 3d1 at $T > 0.002$, and begins to decrease at $T > 0.02$, when the 3d2 subband is also excited.

Upon compression, this maximum decreases in magnitude and shifts towards higher temperatures. We note that γ_e depends little on the temperature ($0 < T < 0.2$) when $1 \leq \delta \leq 3$, and changes in the interval $0.9 < \gamma_e < 1.4$. It should be borne in mind that in calculating $\varphi/2$ for Fe, Ni, and Cu at high temperatures, starting with 0.04, it is necessary to take into account the bands lying above the Fermi surface. Such a band in these metals is 4d.

4. Silver

The energy structure of silver is very similar to the picture of the bands in copper, the only difference being that the upper band is 4d rather than 3d, and the role of 4s is played by 5s. Figure 11 shows a picture of the bands in Ag at $\delta = 1$. The outer electron is in the subband 4d0 ($k_F = 1.919$), and in the s state we have 0.037 electrons, while in the p state we have 0.297 electrons, and in the d state 0.643 electrons. The width of 4d0 in Ag is much larger than the width of the corresponding 3d0 subband in Cu, and therefore the effective mass on the Fermi surface is smaller in

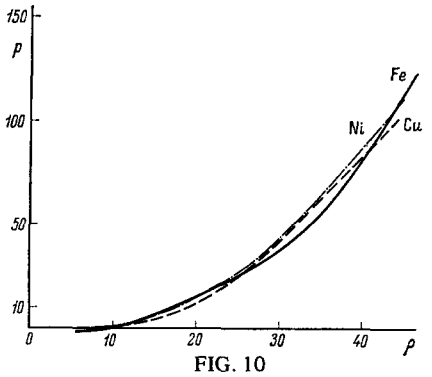

FIG. 10

Table VI. Contributions made to the kinetic pressures by the various bands of Cu

δ	4s	3d0	3d1	3d2
0.75	0.145	0.118	0.314	−0.043
1	0.433	0.262	0.672	−0.033
1.5	1.880	0.929	2.031	0.210
2	4.293	2.231	4.263	0.804
3	11.050	8.626	11.960	3.299
5	44.000	26.944	43.745	15.429

silver than in copper. According to our calculation, the effective mass in Cu is larger by 1.44 times than in Ag, in good agreement with the experimental data[34]. Just as an upward shift of the 4s band is observed in copper upon compression, an analogous shift is observed in Ag for the 5s band. Even at $\delta = 2.5$, the outer electrons are located in 5s and the 4d band strongly overlaps the 5s band.

Figure 12 shows the cold-pressure curve in silver. Calculation yields a value ~22% for the error of the normal density. Table VII illustrates the distribution of the kinetic pressure among the states with different l, and also of the total kinetic pressure among the bands, at $\delta = 1$ and $\delta = 2.5$.

5. Titanium and Vanadium

Interest in Ti and V is due primarily to the fact that their d shells contains few electrons (2 and 3, respectively).

The electron bands calculated by us for titanium are given in Fig. 13 ($\delta = 1.5$) and Fig. 14 ($\delta = 2.0$), where $\delta = \rho/4.5$. Accordingly, the electron structure of vanadium is shown in Fig. 15 ($\delta = 1.5$) and in Fig. 16 ($\delta = 2.0$), where $\delta = \rho/6.08$. Both metals are characterized by an upward shift of the 4s band. Table VIII shows clearly the decrease of the number of electrons in the 4s with decreasing density of either Ti or V.

This abrupt change in the number of electrons occurs in a narrow region of densities. In Ti, the start of the realignment takes place at $\rho \sim 7.9$ g/cm^3, and in V at $\rho \sim 9.1$ g/cm^3, although the value of δ in the realignment region is larger for Ti than in V. The cold-pressure curves $p(\rho)$ of both metals are shown

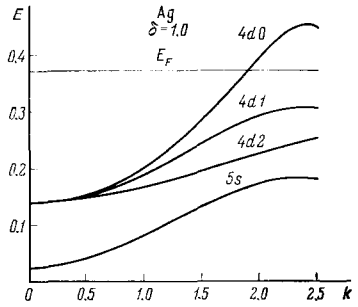

FIG. 11

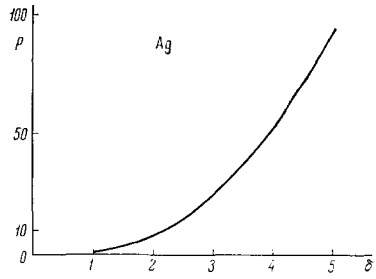

FIG. 12

Table VII

l	δ=1				δ=2.5			
	5s	4d0	4d1	4d2	5s	4d0	4d1	4d2
0	0.128	0.018	—	—	1.25	2.10	—	—
1	0.189	0.172	0.079	—	4.27	1.78	2.11	—
2	−0.158	0.075	0.398	−0.271	0.53	−0.09	5.05	−0.18
3	0.009	0.013	0.035	0.068	0.09	0.14	0.34	0.72
p_{kin}	0.177	0.294	0.582	−0.130	6.24	4.11	8.22	1.20

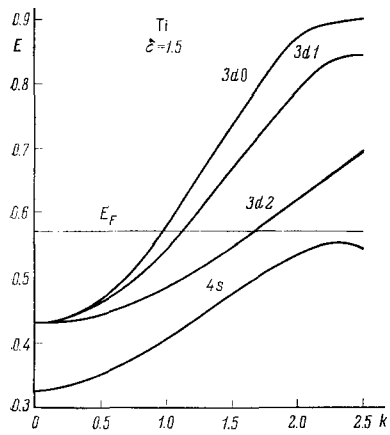

FIG. 13

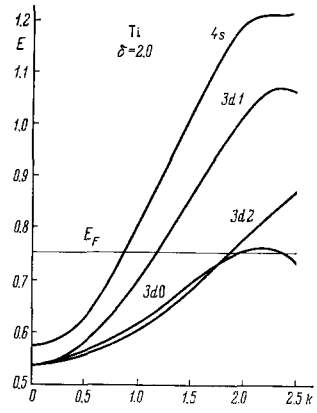

FIG. 14

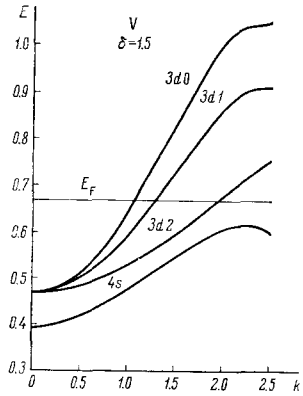

FIG. 15

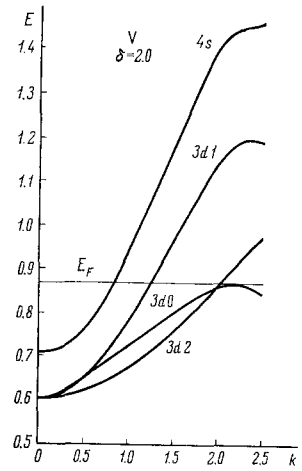

FIG. 16

Table VIII. Number of electrons in bands

δ	Ti				V			
	1,5	1,75	2	3	1,5	1,75	2	3
4s	2	1.938	0.098	—	2	0.131	0.083	—
3d	2	0.062	3.902	4	3	4.869	4.917	5

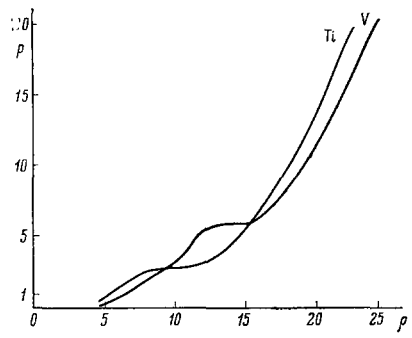

FIG. 17

in Fig. 17. The bend in the indicated region of the electronic realignment is clearly seen in this case.

Table IX shows the contributions made to the kinetic pressure by the bands 4s and 3d.

The subbands 3d1 and 3d2 give a monotonic increase of the kinetic pressure upon compression. A different picture of the behavior of the kinetic pressure takes place in the subband 3d0 and in the band 4s. Whereas the contribution to the kinetic pressure from the 4s band decreases sharply in a narrow region of densities, the contribution of 3d0 increases sharply, i.e., there occurs, as it were, a "transfer of pressure" from 4s to 3d0. Then the pressure in 3d0 decreases, and the principal role in the pressure begins to be played by the subbands 3d2 and 3d1.

Calculations yield different compressibilities for Ti and V. Shock adiabats of Ti and V were recently obtained[24,28]. The shock adiabat of V has a kink at δ = 1.58, and that of Ti has no kink. However, it seems to us that it would be incorrect to conclude therefrom that there is no electron realignment in Ti. In our calculations, the difference between Ti and V was manifest in the fact that the kinetic-pressure curve of Ti is smoother than the corresponding curve for V. As we shall see in the case of Nb, the shock adiabat, while having a small kink, differs noticeably in shape from the cold-pressure curve, owing to the role of the thermal pressures of the electrons and of the lattice. In the case of titanium and vanadium, the different values of the electron Gruneisen coefficient, resulting from the somewhat different character of the electron realignment, lead apparently to a hardly noticeable kink in Ti and a more clearly pronounced kink in V. It seems to us that this is just a case where the absence of a kink in the experimental shock adiabat still does not mean that there is no realignment of the electron bands upon compression of the substance.

In conclusion, we present for comparison the average radii (in Bohr radii) of the different orbits (l = 0, 1, 2) for different degrees of compression on the Fermi surface in Ti and V (Table X).

III. APPENDIX

1. Potassium

A study of the change of the properties of K with changing density has led to certain unexpected results. Recognizing that K can be easily compressed and that agreement with the results of the statistical theory sets in at large degrees of compression, we have carried out calculations for the region of values δ = 0.75, 1, 2, 3, 4, 5, 6, 8, and 10 (see[27]). At normal density, the outer electron of potassium, as expected, is in the 4s band, with k_F = 1.919. The 3p band is very narrow and is far from 4s. The 3d band is above the Fermi energy. Following a threefold compression, the previously unfilled 3d band begins to overlap the 4s band and is partly filled. We shall show later that the anomalous thermal properties of the electrons in K are essentially connected with this overlap. At δ = 5, a change takes place in the arrangement of the bands 4s and 3d, and the 4s band is already on top and is practically unfilled. At δ = 10, the 4s band does not play any role at all in the filling.

Let us proceed to estimate the exchange pressure. For alkali metals, it is well known that the distribution of the electrons is close to uniform. It seemed advisable to us to use a formula expressing the exchange

Table IX

δ		1.5	1.75	2	2.25	2.5	3	3.5
Ti:	4s	2.60	3.35	0.30	0.33	0.20	—	—
	3d0	0.08	0.12	3.10	2.67	2.27	1.82	1.66
	3d1	0.16	0.22	0.39	0.60	0.79	1.16	1.54
	3d2	0.30	0.46	0.95	1.58	2.24	3.73	5.52
V:	4s	3.46	0.36	0.47	0.38	—	—	—
	3d0	0.18	4.49	5.66	5.16	4.35	3.20	3.16
	3d1	0.32	0.44	0.62	0.97	1.33	2.16	2.91
	3d2	0.58	0.91	1.46	2.53	3.74	7.01	10.49

Table X

δ \ l	Ti			V		
	0	1	2	0	1	2
1.5	2.02	1.87	1.66	1.86	1.74	1.44
2	1.80	1.54	1.51	1.55	1.42	1.35
3	1.46	1.14	1.32	1.32	1.04	1.18

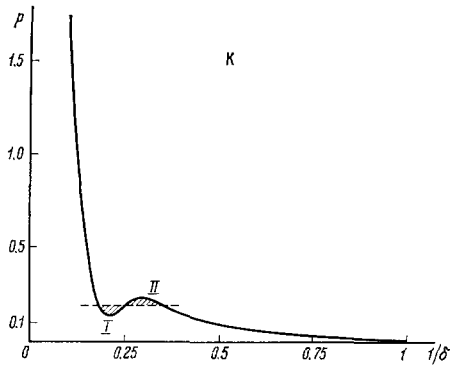

FIG. 18

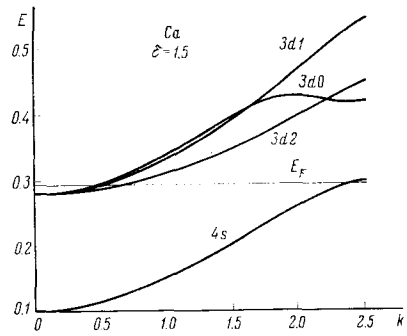

FIG. 19

Table XI

δ	3p	4s	3d
1.5	−0.054 (6)	0.556 (1.9)	0.001 (0.1)
2	−0.081 (6)	0.828 (1.455)	0.085 (0.545)
3	0.016 (6)	0.890 (0.724)	0.449 (1.276)
4	0.459 (6)	0.026 (0.008)	1.425 (1.992)
6	2.630 (6)	—	2.398 (2)

pressure in terms of the electron density. This is the well known formula for exchange pressure in a free electron gas:

$$p_{ex} = -10^4 (Z/28)^{4/3} \rho_e^{4/3} \text{ (in un. of } 10^6 \text{ atm)}.$$

The exchange pressure in K was calculated from this formula, where ρ_e were chosen to be the values of the electron density on the boundary of the cell. Figure 18 shows the dependence of the cold pressure on $1/\delta$. The curve shows a minimum at $1/\delta = 0.21$ and a maximum at $1/\delta = 0.29$. This is evidence of the presence of a first-order transition, and actually a jump of the density is observed at constant pressure. This constant-pressure line is drawn in the figure with allowance for the condition that the areas I and II be equal. This yields a pressure of 0.18 million atm and a large density jump (by a factor of 2). Although the accuracy of the calculation of $p_{ex}(\delta)$ is insufficient to guarantee the correctness of these figures, since this phenomenon is connected with realignment of the electron bands, there is no doubt that such a phase transition is possible. The reliability of the electronic phase transition is verified also by the experimental confirmation, to be discussed later, of the predicted region of negative and small positive electron Gruneisen coefficients connected with the realignment of the bands upon compression.

Stager and Drickamer[36] reported anomalous growth of the electric resistance of potassium in the pressure region under consideration, thus confirming the presence of electron realignment.

We now turn to the data on the thermal properties of the electrons in K. In the region $1 < \delta < 3$, the coefficient $\varphi/2$ depends little on the temperature. At $\delta = 1$ and lower temperatures, the calculated value is $\varphi/2 = 33.58$, which yields $\varphi = 456$ erg/g-deg^2 and is in satisfactory agreement with the experimental value 540 erg/g-deg^2. In the band realignment region, where the 4s and 3d bands overlap, the coefficient $\varphi/2$ depends more strongly on the temperature, decreasing by a factor of 2 when T changes from 0.004 to 0.100. Particularly great interest attaches to the appearance of the region of negative γ_e in the range $2 < \delta < 4$, precisely where electron realignment takes place. Calculations show that the absolute value of γ_e in the negative region decreases with increasing temperature. The reason for the appearance of negative γ_e is that the 3d band begins to overlap the 4s band after compression by a factor 3—4, and this leads to an increase of $\varphi/2$ upon compression. Subsequently, at $\delta > 4$, when 4s is very little filled, γ_e becomes again positive, since the density of the electron levels on the

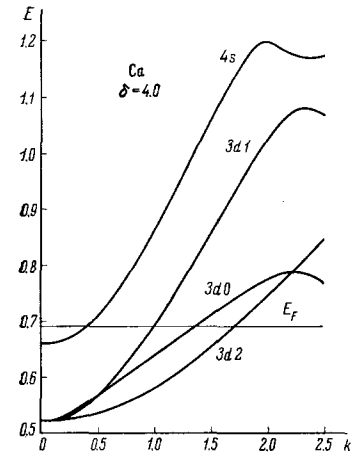

FIG. 20

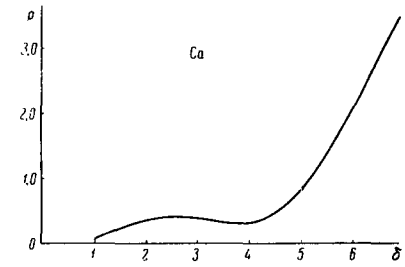

FIG. 21

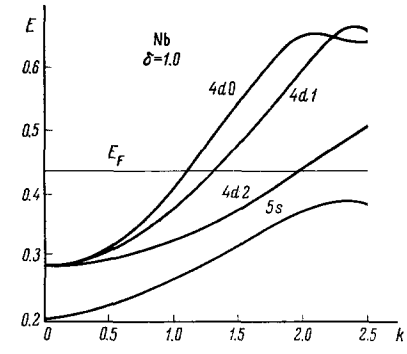

FIG. 22

Fermi surface in the 3d band already decreases with increasing δ.

When the temperature increases to 0.05—0.1 at.un, the calculated value of γ_e reverses sign and assumes the value 0.15 in the interval $2.5 < \delta < 3.5$.

The Hugoniot adiabat calculated from the given values of γ_e and from the extrapolated section of the cold curve is in reasonable agreement with experiment[37]. At the same time, the large starting values ($\gamma_e = 0.5$) of the Gruneisen coefficient of the electrons did not make it possible to interpret unambiguously the dynamic experiment. All this shows that knowledge of the changes of the structure of the energy bands of metals upon compression is essential for the interpretation of the data of the dynamic experiment. The success of the theory in the interpretation of the dynamic experiment increases the reliability of the predictions of the phase transition in K.

2. Calcium

In the Ca atom the configuration is $1s^2 2s^2 2p^6 3s^2 3p^6 4s^2$ and the ground term 1S. Therefore the metallic properties of potassium can result from the overlap of the 4s and 3d bands. Many calculations were performed (δ = 1, 1.5, 2, 2.25, 2.5, 2.75, 3, 3.5, 4, 4.3, 4.5, 4.8, 5, 5.5, 6, and 7) which made it possible not only to establish the transition of the electrons to the 3d band, but also to analyze in detail the electron realignment, which, just as in K, consists in the fact that the states in the 4s band, starting with $\delta = 4$, are not filled with increasing compression ("departure of the 4s band"). Owing to the inaccuracy of the method, we were unable to obtain a normal density overlap of the 3d and 4s bands. The gap between these bands at $\delta = 1$ is 0.074 at.un.

Figure 19 ($\delta = 1.5$) shows the position of the upper bands in Ca, when the width of the energy overlap of 3d and 4s amounts to 0.014. It is seen from Table XI that the number of electrons in the 3d band is 0.1. With further compression, the number of electrons in 3d increases, and the 4s band tends to rise above the Fermi energy, so that at $\delta > 4$ it no longer takes part in the filling. One of the stages of this process is seen in Fig. 20.

Figure 21 shows $p(\delta)$ (cold pressure). We see here clearly a region of almost constant pressure, connected with the aforementioned realignment. In Table XI are given the contributions from different bands to the kinetic pressure in Ca. The numbers in the parentheses are the electronic occupation numbers.

It can be established that the main contribution to the pressure is made by the electrons in the s- and p-states. It is seen from the table that starting with $\delta \sim 4$ the contribution to the pressure from the 3p band increases sharply. This is a consequence of the fact that at such degrees of compression the gap between the 3d and 3p bands decreases strongly (at $\delta = 4$ the gap is equal to 0.398 at.un., at $\delta = 7$ the gap is 0.116 at.un.) Upon subsequent compression, a new realignment of the bands takes place, and the 3p band turns out to be higher in energy than the 3d band. The electrons previously in the 3p band occupy vacant places in the 3d band.

Measurements of the energy structure of Ca upon compression could not fail to influence the behavior of γ_e. In view of the fact that we have described in detail the connection between the electron realignment and the behavior of the electronic Gruneisen coefficient in K, we note only that the dependence of γ_e on the density and temperature is similar in Ca and in K.

3. Niobium

The electronic structure of the transition metals of the fifth period of the periodic system and its change upon compression will be illustrated with Nb as an example. The calculations were performed in the region $0.75 \leq \delta \leq 5$. In the Nb atom, 28 inner electrons form a closed shell $1s^2 2s^2 2p^6 3s^2 3p^6 3d^{10}$, and the remaining 13 electrons are at the levels 4s, 4p, 4d, and 5s. The levels 4s and 4p are completely filled. According to data[2], the 5s level is deeper than 4d. In Nb metal ($\rho_0 = 8.58$ g/cm^3) at normal density (Fig. 22), an energy overlap of the bands 5s and 4d

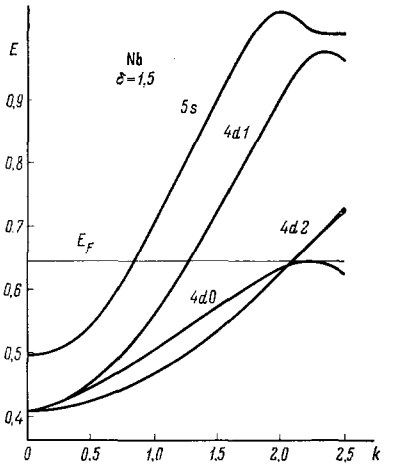

FIG. 23

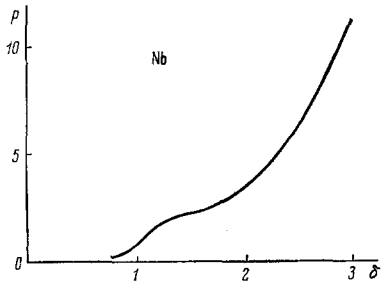

FIG. 24

Table XII

	δ=1		δ=1,5		δ=2	
	n	p_{kin}	n	p_{kin}	n	p_{kin}
5s	2,000	1.175	0.086	0.209	0.001	0,008
4d0	0.192	0.060	1.712	2.364	0.866	1.985
4d1	0.635	0.117	0.578	0.359	0.600	0,900
4d2	2.173	0.191	2,624	0,893	3.533	2,912

takes place, and the Fermi surface intersects only the 4d band. Just as in the case of other transition metals, electron realignment is observed in Nb upon compression: first the overlap of the bands 5s and 4d increases, and then the 5s band turns out to be higher than the Fermi energy. Figure 23 and the electronic occupation numbers listed in Table XII clearly demonstrate this process.

In Table XII are given also the contributions of the bands to the kinetic pressure. Although at $\delta = 1$ the 5s band lies lower than the Fermi energy, the pressure in it is much higher than the pressure in the 4d band. Subsequently, the contribution of 5s to the pressure decreases rapidly, this being connected with the already described electron realignment.

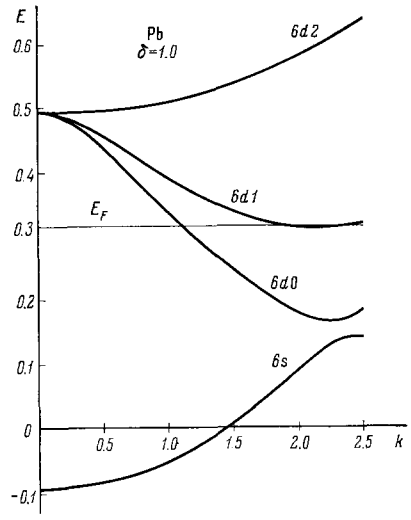

FIG. 25

The cold-pressure curve (Fig. 24) has a noticeable inflection in the region $1 < \delta < 1.75$.

The most characteristic of the thermal properties of Nb is the presence of large values of the electronic Gruneisen coefficient in a wide range of densities and temperatures, which is also connected with the indicated change of the energy structure. This causes the shock adiabat to deviate strongly from the cold-pressure curve to the left at $\delta \leq 1.5$, and near $\delta = 1.5$ there is a characteristic kink of the adiabat.

4. Lead

It is of considerable interest to investigate the equations of state of heavy elements. Greatest attention is paid in this case to Pb, distinguishing features of which are the large compressibility of the relatively low normal density (11.4 g/cm^3). Calculations of the electronic spectrum for Pb were made at the following values of δ: 0.75, 1.0, 1.5, 2.0, 3.0, and 5.0.

Lead has four electrons on top of the filled configuration $1s^2 2s^2 2p^6 3s^2 3p^6 3d^{10} 4s^2 4p^6 4d^{10} 4f^{14} 5s^2 5p^6 5d^{10}$, which consists of 78 electrons. These four electrons are distributed in the bands 6s and 6d. It is seen from Fig. 25, that at $\delta = 1$ the 6s band is filled. The two other electrons are in the 6d band, with only 0.206 electrons in the 6d1 subband. However, in spite of the designation 6d, in fact the greater part of the electrons in this band are in s- and p-states. Table XIII for the relative degrees of compression $\delta = 1$ and $\delta = 3$ clearly confirms this fact. Indeed, out of the two electrons of the 6d band, 1.3 are in the p state and 0.43 in

Table XIII

	l	$\delta=1$				$\delta=3$			
		0	1	2	3	0	1	2	3
n_e	6d0	0.427	1.133	0.089	0.106	0.591	0.258	0.280	0.321
	6d1	—	0.164	0.005	0.027	—	0.304	0.013	0.161
p_e	6d0	0.128	0.110	0.041	0.031	1.752	0.782	1.166	0.513
	6d1	—	0.034	0.002	0.008	—	0.999	0.064	0.268

Table XIV. Dependence of the pressure on the density of Pb

δ	W	p_{ex}	p_{kin}	p	δ	W	p_{ex}	p_{kin}	p
0.75	0.220	—0.152	0.204	0.052	2.00	0.649	—1.326	3.832	2.506
1.00	0.302	—0.287	0.510	0.223	3.00	1.001	—3.159	12.467	9.308
1.50	0.470	—0.697	1.590	0.893	5.00	1.745	—9.596	52.629	43.033

Table XV. Contributions of the individual bands to the kinetic pressure in Pb

δ	5d	6s	6d0	6d1	δ	5d	6s	6d0	6d1
0.75	—0.021	0.037	0.144	0.044	2.00	—0.001	1.506	1.888	0.438
1.00	—0.056	0.131	0.332	0.103	3.00	1.928	4.715	4.352	1.472
1.50	—0.146	0.608	0.948	0.180	5.00	16.750	18.190	8.430	9.260

the s state. The arrangement of the bands at $\delta = 1$ is conserved in the entire range of relative compressions. To be sure, many more electrons are in the states with $l = 2$ and 3 already at $l = 3$, and this increases the number of electrons in the subband 6d1.

Tables XIV and XV give data on the cold pressure in lead.

The main feature of Pb, the very large compressibility, is well described theoretically. At a compression by two times, the pressure in Pb is 2.5 million atm, whereas in Cu^-, Fe, and in Ni it is 8 million, 7.4 million, and 10.5 million atm. respectively at the same twofold compression.

Calculation at $\delta = 1$ yielded a pressure of 0.223 million atm, i.e., a rather small value. The error in the normal density is approximately 30%, and the calculated density at $p = 0$ is even smaller than the experimental value $\rho_0 = 11.4$ g/cm^3. Although Pb is a heavy element, the s and p electrons in the 6d band can be easily compressed. In Table V we give the contributions made to the kinetic pressure by states with different $l(p_l)$ in the subbands 6d0 and 6d1. As always, the relative role of the s states is largest here.

[1] R. Feynman, N. Metropolis, and E. Teller, Phys. Rev. 75, 1561 (1949).
[2] R. Latter, Phys. Rev. 99, 1854 (1955).
[3] D. A. Kirzhnits, Zh. Eksp. Teor. Fiz. 32, 115 (1957) [Soviet Phys.-JETP 5, 64 (1957)].
[4] D. A. Kirzhnits, ibid. 35, 1545 (1958) [8, 1081 (1959)].
[5] N. N. Kalitkin, ibid. 38, 1534 (1960) [11, 1106 (1960)].
[6] L. V. Al'tshuler, K. K. Krupnikov, B. N. Ledenev, V. I. Zhuchikhin, and M. I. Brazhnik, ibid. 34, 874 (1958) [7, 606 (1958)].
[7] A. A. Abrikosov, Astron. Zh. 31, 112 (1954).
[8] W. Carr, Phys. Rev. 128, 120 (1962).
[9] R. Sternheimer, Phys. Rev. 78, 235 (1950).
[10] I. M. Lifshitz, Zh. Eksp. Teor. Fiz. 38, 1569 (1970) [Soviet Phys.-JETP 11, 1130 (1960)].
[11] F. Seitz, Modern Theory of Solids, New York, 1940.
[12] F. Herman, Revs. Modern Phys. 30, 102 (1958).
[13] J. Reitz, Solid State Phys. 1, 1 (1955).
[14] J. Callaway, Energy Band. Theory, Academic Press, New York, 1964.
[15] D. Hartree, Calculations of Atomic Structures (Russ. transl.), I.L., 1960.
[16] R. Reynman, Phys. Rev. 56, 340 (1939).
[17] N. A. Dmitriev, Zh. Eksp. Teor. Fiz. 42, 772 (1962) [Sov. Phys.-JETP 15, 539 (1962)].
[18] G. M. Gandel'man, ibid 43, 131 (1962) [16, 94 (1963)].
[19] L. V. Al'tshuler, A. A. Bakanova, and I. P. Dudoladov, ZhETF Pis. Red. 3, 483 (1966) [JETP Lett. 3, 315 (1966)].
[20] L. V. Al'tshuler, A. A. Bakanova, and I. P. Dudoladov, Zh. Eksp. Teor. Fiz. 53, 1967 (1967) [Sov. Phys.-JETP 26, 1115 (1968)].
[21] R. Duff, W. Gust, E. Royce, A. Mitchell, R. Keeler, and W. Hoover, Symposium High Dynamic Pressure, Paris, 1967.
[22] R. G. Arkhipov, Zh. Eksp. Teor. Fiz. 49, 1601 (1965) [Sov. Phys.-JETP 22, 1095 (1966)]; Fiz. Tverd. Tela 4, 1077 (1962) [Sov. Phys. Solid State 4, 795 (1962)].
[23] E. S. Alekseev, Dissertation, Crystallography Institute, USSR Academy of Sciences, 1969.
[24] K. K. Krupnikov, A. A. Bakanova, M. I. Brazhnik, and R. F. Trunin, Dokl. Akad. Nauk SSSR 148, 1302 (1963) [Sov. Phys.-Dokl. 8, 203 (1963)].
[25] S. B. Kormer, A. I. Funtikov, V. D. Urlin, and A. N. Kolesnikova, Zh. Eksp. Teor. Fiz. 42, 686 (1962) [Sov. Phys.-JETP 15, 477 (1962)].
[26] G. M. Gandel'man, Dissertation, Institute of Physics Problems, USSR Academy of Sciences 1966.
[27] G. M. Gandel'man, Zh. Eksp. Teor. Fiz. 51, 147 (1966) [Sov. Phys.-JETP 24, 99 (1967)].
[28] G. M. Gandel'man, ibid. 48, 758 (1965) [21, 501 (1965)].
[29] G. M. Gandel'man, V. M. Ermachenko, and Ya. B. Zel'dovich, ibid. 44, 386 (1963) [17, 263 (1963)].
[30] W. Pauli, General Principles of Quantum Mechanics, (Russ. transl.) Gostekhizdat, 1947, pp. 46–61.
[31] L. V. Al'tshuler, and A. A. Bakanova, Usp. Fiz. Nauk 96, 193 (1968) [Sov. Phys. Usp. 11, 678 (1969)].
[32] J. Skidmore and E. Morris, Proceedings of Symposium, Vienna, 1962.
[33] B. Segall, Phys. Rev. 125, 109 (1962).
[34] H. Ehrenreich,and H. Phillipp, Phys. Rev. 128, 1622 (1962).
[35] B. Segall, Phys. Rev. 124, 1797 (1961).
[36] R. A. Stager and H. G. Drickamer, Phys. Rev. 132, 124 (1963).
[37] A. A. Bakanova, R. F. Trunin, and P. P. Dudoladov, Fiz. Tverd. Tela 7, 1615 (1965) [Sov. Phys. Solid State 7, 1307 (1965)].

Translated by J. G. Adashko